

DETERMINATION OF THE SMOKE-PLUME HEIGHTS WITH SCANNING LIDAR USING ALTERNATIVE FUNCTIONS FOR ESTABLISHING THE ATMOSPHERIC HETEROGENEITY LOCATIONS

Vladimir A. Kovalev, Alexander Petkov, Cyle Wold, and Wei Min Hao

U.S. Forest Service, RMRS Fire Sciences Laboratory, Missoula, MT 59808, USA, E-mail: vkovalev@fs.fed.us

ABSTRACT

Data-processing techniques for the scanning lidar data are considered that allow determining the upper and lower boundaries of the smoke plume or smoke layering in the vicinity of wildfires. The task is fulfilled by utilizing the Atmospheric Heterogeneity Height Indicator (AHHI). The AHHI is a histogram, which shows a number of heterogeneity events defined by scanning lidar at the consecutive height intervals in a heterogeneous atmosphere. Different variants of creating the AHHI plots for investigating the atmospheres contaminated with the smoke plume are considered. Because the boundaries of the dispersed smoke plume are often not well defined, user-defined criteria are considered, which allow utilizing the automatic data processing procedure. The smoke boundary height is defined as the location where a special function, determined from the scanning lidar signals, varies within acceptable limits, and the standard deviation of the calculated height does not exceed an established value.

The best results are achieved when different variants of the AHHI are used to determine the upper and the lower height of the smoke plume.

1. INTRODUCTION

Scanning lidar is the most practical tool for the investigation of wildfire smoke-plume dynamics and heights. It allows continuous monitoring of diurnal and spatial variation of aerosol properties and dynamics in smoky-polluted atmospheres.

Recently the methodology for investigation of smoke plume rise and dispersion with scanning lidar was considered, where the concept of the Atmospheric Heterogeneity Height Indicator (AHHI) was introduced [1]. The AHHI is a histogram, which shows a number of heterogeneity events defined by the lidar in the consecutive height intervals of the searched area when making vertical scan. It defines both the heights at which the increased smoke-plume heterogeneity occurs and the number of the heterogeneity events observed at these heights.

In this study, we analyze possible techniques for creating the AHHI plots when investigating the atmospheres contaminated with smoke plume. In all cases considered below, the lidar signals at the wavelength 1064 nm were processed.

2. CALCULATION TECHNIQUES FOR CREATING THE ATMOSPHERIC HETEROGENEITY HEIGHT INDICATOR

The basic principle of determining the atmospheric heterogeneity location with the AHHI is similar to any other method of determining heterogeneity; that is, the areas where increased gradients in the backscatter signal exist are identified. At least five alternative functions can be used to create the AHHI plots.

(a) AHHI-1 computed by transforming the conventional Range-Height-Indicator (RHI)

In this variant, the square range-corrected backscatter signals, measured with the scanning lidar along the consecutive slope directions, φ , are calculated; i.e.,

$$P(r_\varphi)r_\varphi^2 = [P_\Sigma(r_\varphi) - B]r_\varphi^2. \quad (1)$$

Here $P_\Sigma(r_\varphi)$ is the recorded lidar signal, which is the sum of the range-dependent backscatter signal, $P(r_\varphi)$ at the range r_φ and the range independent offset, B . For the determination of the AHHI, the absolute values of the square range-corrected backscatter signals, taken as a function of the height, $h = r_\varphi \sin \varphi$, are used,

$$F_1(h, \varphi) = \left| P(r_\varphi)r_\varphi^2 \right|. \quad (2)$$

(b) AHHI-2 computed by using the sliding derivative of the square-range-corrected signal

In this variant, the sliding derivative of the square-range-corrected signal, $P(r_\varphi)r_\varphi^2$, measured with lidar along the direction φ is calculated. For the determination of the AHHI-2, the absolute values of the derivative, taken as a function of the height, h , are used,

$$F_2(h, \varphi) = \left| \frac{d}{dr_\varphi} \left[P(r_\varphi) r_\varphi^2 \right] \right|. \quad (3)$$

(c) AHHI-3 computed by using the sliding derivative dY/dx

The function $Y(x)$ is obtained by transforming the recorded lidar signal in the form [1],

$$Y(x) = P_\Sigma(x)x = [P(x) + B]x, \quad (4)$$

here $x = r^2$. The derivative of $Y(x)$ with respect to x is,

$$\frac{dY_\varphi}{dx_\varphi} = \frac{d[P(x_\varphi)x_\varphi]}{dx_\varphi} + B. \quad (5)$$

The product $P(x_\varphi)x_\varphi$ is the square-range-corrected backscatter signal at $x_\varphi = r_\varphi^2$. For the calculation of the AHHI-3, the absolute value of the difference of dY/dx versus height and the offset is used,

$$F_3(h, \varphi) = \left| \frac{d}{dx_\varphi} \left[Y_\varphi(h) \right] - B_\varphi \right|. \quad (6)$$

The offset B_φ can be found by determining the derivative, $d/dx_\varphi[Y_\varphi(h)]$ over the distant ranges where the backscatter signal, $P(x_\varphi) \rightarrow 0$.

(d) AHHI-4 and AHHI-5 computed using the intercept points of the slope of the function Y_φ

For the determination of these functions, the intercept point of the slope of the function Y_φ with the vertical axis is found. For determining AHHI-4, the non-normalized intercept function,

$$Y_0(x, \varphi) = Y_\varphi - \frac{dY_\varphi}{dx_\varphi} x_\varphi, \quad (7)$$

is used. For determining AHHI-5, the normalized intercept function, defined as

$$Y_{0,norm}(x, \varphi) = \frac{Y_0(x, \varphi)}{x_\varphi + \Delta_\varphi}, \quad (8)$$

is used. Here Δ_φ is a user-defined positive non-zero constant, whose value can be chosen within the range $(0.02 - 0.05)x_{\varphi, \max}$; $x_{\varphi, \max}$ is the maximum of x_φ over the selected height interval [1]. Similar to the previous case, the absolute values of these functions versus height are used for determining AHHI-4 and AHHI-5,

$$F_4(h, \varphi) = |Y_0(h, \varphi)|, \quad (9)$$

$$F_5(h, \varphi) = |Y_{0,norm}(h, \varphi)|. \quad (10)$$

Note that the determination of AHHI-4 and AHHI-5 does not require the estimate and the removal of the shift B in the recorded lidar signal.

3. DETERMINATION OF THE SMOKE PLUME HEIGHTS USING ATMOSPHERIC HETEROGENEITY HEIGHT INDICATOR

The procedure for computation of the AHHI for all variants is similar. Initially, the functions $F_i(h, \varphi)$ for each slope direction φ are determined and their average, $F_{i,aver}(h)$, is calculated. Then the maximum function, F_{max} for the above set of the functions is found. The local heterogeneity event is considered as being true at the locations where the function $F_i(h, \varphi)$ reaches some established, user-defined level, χ , relative to F_{max} [1].

An example of such an AHHI plot, obtained with the function $F_3(h, \varphi)$ from the signals of the vertically scanning lidar in a smoky polluted atmosphere is shown in Fig. 1. The number of heterogeneity events, $n(h)$, determined for the consecutive height intervals, is shown with the filled squares. One can see that the upper boundary of the smoke is located close to the height of ~ 2500 m. However, isolated heterogeneity events are also fixed within the height interval from 3000 m to 4100 m.

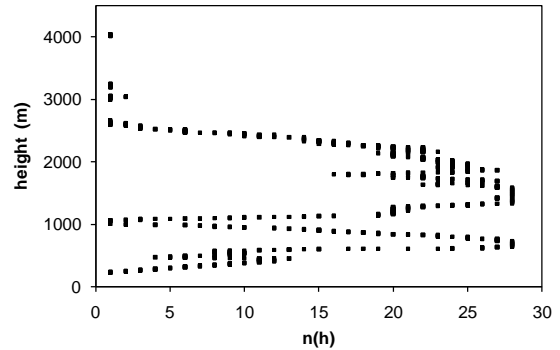


Fig. 1. AHHI-3 plot, obtained from the signals measured by a vertically scanning lidar in a smoke polluted atmosphere.

A frequent issue in the determination of the smoke plume height is establishing whether the fixed heterogeneity events, such as at the above heights 3000-4100 m, are real, or originated in the signal noise. Note also that data-points originated in the local heterogeneity, generally, are beyond our study interest. Therefore, isolated or randomly distributed $n(h)$ are excluded from our analysis.

In our previous study [1], the heterogeneity locations were determined as the heights where $F_i(h, \varphi) \geq \chi F_{max}$, with $\chi < 1$. However, the general question of what values of $n(h)$ can be ignored and what values can not, should be answered. To clarify this issue, let us consider the dependence of the height of the upper smoke boundary, $h_{sm,up}$ on the selected χ for AHHI-3 shown in Fig. 1. Such a dependence of $h_{sm,up}$ on the discrete χ , taken within

the range of χ from 0.1 to 0.5 with the step 0.05 is shown in Fig. 2 with the filled squares. One can see that the selection of $\chi = 0.1$ yields $h_{sm,up} \sim 4000$ m, and that increasing χ results in the sharp decrease of the height down to the more realistic height of ~ 2500 m. Similarly, analysis along another azimuthal direction, shifted by 10° , again shows a large $h_{sm,up}$ located between 4000 m and 5000 m when the values for χ equals 0.1, 0.15, and 0.2, are used.

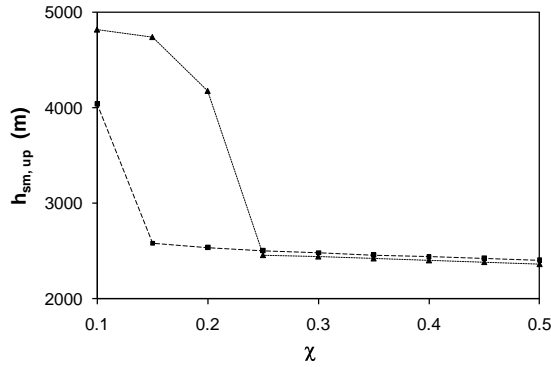


Fig. 2. The height of the upper smoke boundary versus selected χ for two azimuthal directions shifted by 10° relative of each other.

Thus, the selection of χ for determining the location of the smoke boundary is an issue. Moreover, there is no commonly accepted definition of the boundary of the heterogeneity, where no sharp, well-defined transition from the polluted area to clear air takes place. Therefore, selecting the definition of the smoke-plume boundary remains a prerogative of the researcher; it can only be done during analysis of the experimental data.

Two basic requirements should be met when determining the boundary of dispersed smoke. First, the retrieval technique must be consistent for the entire set of the analyzed data. Second, there should be criteria for rejecting unreliable or suspicious results. To meet the latter requirement, we apply the following procedure. We determine the smoke boundary using some number of the discrete and consecutive χ rather than a single value of χ . Particularly, in our calculations, we use the discrete values from $\chi_{min} = 0.2$ to $\chi_{max} = 0.5$, with the step 0.05. Beginning with χ_{min} , we find the corresponding value of the smoke-boundary height, and then calculate the mean value of the height and its standard deviation (STD). The value of the mean is considered the trustworthy smoke-boundary height if its standard deviation does not exceed 10% of the mean height. Otherwise, χ_{min} is increased up to the next discrete value and the values of the mean and the STD are recalculated with the same χ_{max} . If the relative error still exceeds 10% of the newly

calculated mean boundary height, χ_{min} is increased up to the next discrete value. The procedure is repeated until the level of 10% for the STD of the mean is achieved. If this is not achievable, the measurement results from this scan are either not taken into consideration, or are analyzed using more sophisticated criteria.

For the first data set, shown in Fig. 2 as the filled squares, the mean for the discrete χ taken from 0.2 to 0.5 is 2464 m, and its STD = 46 m, that is 1.9%. For the second, shown as the filled triangles, the mean and STD taken under the same conditions, are 2663 m and 668 m, respectively. As the relative error exceeds 10%, the above correction procedure is made. The increase of χ_{min} up to 0.25 yields a mean equal to 2411 m and a STD equal to 36 m, that is, 1.5%. Accordingly, the difference in the top boundary heights determined for these azimuthal directions is 53 m, which is close to both values of STD.

4. DISCUSSION AND SUMMARY

When measuring wildfire smoke plumes, different situations can be encountered. Accordingly, the most appropriate lidar data-processing variants should be applied, depending on the spatial location and the spread of smoke polluted areas. We identified five typical situations met during our multi-year lidar measurements: (1) Vertical smoke plume over relatively restricted area of intense burning (Tripod Complex Fire, Okanogan, Washington, 2006; LeHardy Fire, Wyoming, 2008). (2) Highly dispersed smoke haze in the lower troposphere monitored in the vicinity of large fires (Tripod Complex Fire, Winthrop, Washington, 2006). (3) Separate local fire plumes scattered within some wildfire area (GILA WFU incident in New Mexico, 2005). (4) Horizontally stratified smoke layers at different heights, generally at distances more than 10 -15 miles from the active flaming area, often created by numerous scattered fires (I-90 Fire, Montana, 2005), and (5) Smoke plume close to active wildfire area spreading downwind (Kootenai Creek Fire, Montana, 2009).

Different requirements for the retrieved data should be made when determining smoke-plume dynamics in different situations. For the cases 1, 2, and 3, only the maximal smoke-plume heights and their temporal changes are required to be monitored. For the cases 4 and 5, both the upper and lower heights of the smoke plume are often parameters of interest. Accordingly, different variants of the AHHI should be used in such different situations.

In this study, we investigated the most general case where information is required for both

the upper and the lower heights of the smoke plume. For the analysis, we utilized the lidar data measured during the Kootenai Creek Fire in Montana. Using these data, all the alternative functions [$F_1(h, \varphi)$, $F_2(h, \varphi)$, $F_3(h, \varphi)$, $F_4(h, \varphi)$, and $F_5(h, \varphi)$] were investigated, and the corresponding AHHI plots were built and analyzed.

The schematic of the data collection with the vertically scanning lidar during the Kootenai Creek Fire on August 27, 2009, is shown in Fig. 3. The wildfire occurred in a wild mountainous area from which the smoke plume spread in an Easterly direction, to the valley where the lidar was located. The height of the lidar site was approximately 900 m below the height where the wildfire took place. The lidar vertical scans were made along 23 azimuthal directions, from 45° to 155° with the angular separation 5° . Each vertical scan yielded a cross-section of attenuated backscatter in the fixed azimuthal direction. From each scan, the smoke plume heights were determined using dependencies like those shown in Fig. 2. The results from determining the upper and lower heights for the above azimuthal directions, measured from 12:09 PM to 12:28 PM are presented in Fig. 4. The heights of

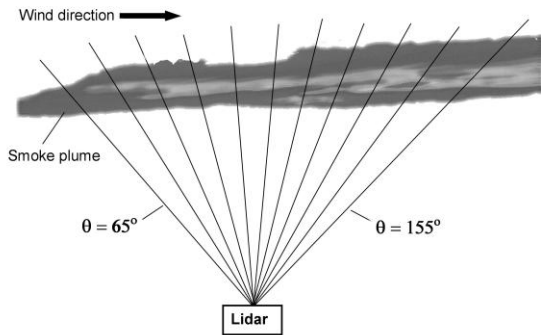


Fig. 3. Schematic of the lidar deployment. The thin lines show the scanned azimuthal directions. (The sector $45^\circ - 65^\circ$, which overlaps the wildfire site, is not shown in the figure).

the upper boundaries determined with AHHI-5 are shown as the filled triangles. The lower heights, determined with AHHI-4, are shown as the filled diamonds. One can see that for the searched azimuthal direction, the height of the upper boundary varies in space less than the height of the lower boundary. Note also that both heights tend to decrease as the smoke moves away from the wildfire location until making contact with the top of the boundary layer, shown as the filled circles.

Different issues are met when determining the lower and the upper boundaries of the smoke

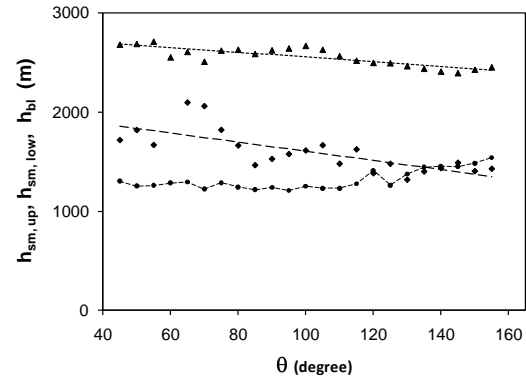


Fig. 4. The heights of the upper and lower smoke plume boundaries of the Kootenai Creek Fire on August 27, 2009 (the filled triangles and the filled diamonds, respectively) versus searching azimuthal directions, and their linear fit. The filled circles show the height of the boundary layer.

plume. The determination of the upper boundary is complicated by random noise, which often enormously increases at the far end of the measured range when the square range correction is made. This feature is especially observable when AHHI-1 and AHHI-2 are used to determine the upper boundary. For the lower boundary, the main issue is to find the location of the transition zone between the top of the polluted air of the boundary layer and the bottom of the smoke plume. In some cases, the automatic processing of the lidar data does not discriminate these areas, especially in a multilayered atmosphere.

The use of AHHI-3 and AHHI-5 tend to yield closely related results, and are most applicable for determining the upper boundary of the smoke plume. For the analyzed data of the Kootenai Creek Fire, AHHI-5 yielded less scattered data than AHHI-3; therefore, we present here the heights of the smoke upper boundary, obtained with AHHI-5. AHHI-4 minimizes the influence of the polluted air in the boundary layer when determining the lower height of the smoke plume. Therefore, it is the best choice for determining the lower smoke boundary.

The multi-layering atmosphere requires a more sophisticated processing procedure. In this case, appropriate height intervals within the total measured range should be established and analyzed separately.

5. REFERENCES

- [1] V. A. Kovalev, A. Petkov, C. Wold, S. Urbanski, and W. M. Hao, "Determination of smoke plume and layer heights using scanning lidar data," Appl. Opt., **48**, 5287-5294, 2009.